

The survey of climatic drought trend in Iran

Hossein Bari Abarghouei · Mohammad Amin Asadi Zarch ·
Mohammad Taghi Dastorani · Mohammad Reza Kousari ·
Mehdi Safari Zarch

Published online: 27 April 2011
© Springer-Verlag 2011

Abstract Drought is one of the most important natural hazards in Iran. Therefore, drought monitoring has become a point of concern for most of the researchers. In the present study, the changes and trend of drought was surveyed, under the current global climate changes, by non parametric Mann–Kendall statistical test for 42 synoptic stations at different places of Iran. Standardized Precipitation Index (SPI) was calculated to recognize the drought condition at different time scales (3, 6, 9, 12, 18 and 24 months' time series) for analyzing the drought trend in the recent 30 years. The obtained results have indicated a significant negative trend of drought in many parts of Iran, especially the South-East, West and South-West regions of the country. According to the results, although some parts of Iran such as North (around the Caspian Sea) and Northeast show no significant trend but in other parts of country, the severity of drought has increased during the last 30 years.

Keywords Drought · Climate ·
Standardized Precipitation Index · Survey

H. Bari Abarghouei · M. Safari Zarch
Department of Agriculture, Payame Noor University, Yazd, Iran

M. A. Asadi Zarch (✉)
Faculty of Natural Resources, Yazd University, Yazd, Iran
e-mail: amin_asadi@ymail.com

M. T. Dastorani
Faculty of Natural Resources, Yazd University, Yazd, Iran

M. R. Kousari
Management Center for Strategic Projects, Fars Organization
Center of Jihad Agriculture, Shiraz, Iran

1 Introduction

Drought is usually defined as a significant temporary reduction in water availability below the expected amount for a specified period and for a particular climatic zone (Bonaccorso et al. 2003). Droughts are one of the normal and recurrent climatic phenomena on earth. However, recurring prolonged droughts have caused far-reaching and diverse impacts because of water deficits (Nadarajah 2009). Droughts differ from other natural hazards, such as floods, tropical cyclones, and earth quakes in several ways. First, since the effects of a drought often accumulate slowly over a considerable period of time that may longer for several years even after the termination of drought, it is difficult to precisely determine the onset and end of a drought event. This is the reason that a drought is often referred to as a creeping phenomenon (Mishra et al. 2009).

Drought is considered to be an extreme climatic event causing significant damage both in the natural environment and in human lives (Modarres 2007). Drought is amongst the world's costliest disasters and affects a very large number of people every year (Wilhite 2000). On the other hand, Drought is one of the most important natural hazards in Iran and always affects a large number of people while causing tremendous economic losses, environmental damage and social hardships in different regions of country. In Iran, drought has always caused degradation in quantity and quality of farm products, agricultural output and farmers' living standard. Shortage of water and rainfall causes a significant reduction in cultivated area and food production. For example, drought in 1998 destroyed almost 200000 hectares of horticultural lands in Iran (Soleimmi et al. 2005; Yazdani and Kianirad 2004). Therefore, the survey of climatic drought trend in Iran, especially under current global climate changes, is one of the most

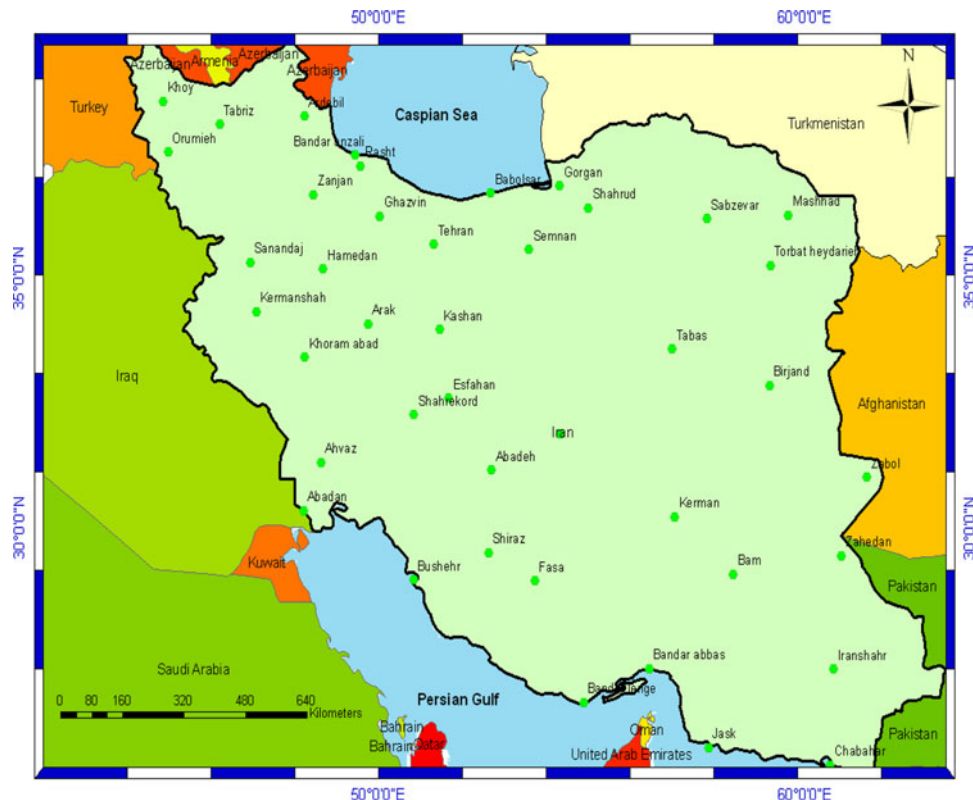
important subjects and it is necessary to analyze the characteristics of this important climatic parameter.

The definition and identification of drought has been an objective of many research efforts for a long time (Łabędzki 2007). Drought has been sorted into four types (Wilhite and Glantz 1985): meteorological, agricultural, hydrological, and socio-economical. In a practical way, there is no universally accepted definition of drought (Tate and Gustard 2000). Recent investigations show that drought should be defined as a natural but temporary imbalance in water availability, consisting of a persistent lower-than average precipitation, resulting in diminished availability of water resources (Paulo and Pereira 2006). Most definitions attribute drought to be a breakdown in the rainfall regime. Meteorological drought, lasting sufficiently to cause hydrological and agricultural hazards, is expressed in terms of rainfall in relation to an average amount and the duration of a dry period and can be defined as a period with the lack of precipitation or lower-than-average rainfall (Zhai and Feng 2008).

During the past decade, a significant amount of research has been carried out on the drought characteristics, especially in Iran. Morid et al. (2006) has examined the performances of seven drought indices requiring only rainfall data for drought detection and monitoring in the Tehran province of Iran. They have concluded that the SPI and Effective Drought Index (EDI) could be recommended for the operational drought monitoring in a region; however,

the EDI requires daily precipitation that constitutes a serious limitation for its operational use. Akhtari et al. (2009) used several geostatistical methods for the derivation of draught-index maps. The tests were evaluated using 1-month SPI and EDI at 43 climatic stations in the Tehran province of Iran. According to their results, although the kriging is the most accurate method, but weighted moving average provides a reasonable accuracy combined with the simplicity and speed of the procedure. For determining the relationship between regionalization of precipitation regimes in Western Iran and the regional drought variability, Raziei et al. (2008) have suggested that the Precipitation Index did not prove to be a proper index for drought analysis due to its shortcomings. While, the SPI technique appeared to be more suitable. But the SPI technique used for assessing the drought variability in Iran proved to be appropriate (Raziei et al. 2009). During the study of Raziei et al. (2009), the analysis was limited to the Western Iran for the period of 1966–2000 and only NCEP/NCAR and rain gauge observations were considered. While the same author has applied GPCP and NCEP/NCAR database for the analysis of drought variability in Iran (Raziei et al. 2010). Rahimzadeh Bajgirani et al. (2008) used the Normalized Difference Vegetation Index (NDVI) and Vegetation Condition Index (VCI) and correlated their values to the precipitation data for evaluating the capability of NOAA-AVHRR data for drought monitoring in the Northwest Iran.

Fig. 1 Distribution of 42 surveyed synoptic stations in Iran



The most commonly used procedures for drought monitoring are Palmer Drought Severity Index (PDSI; Palmer 1965) and the Standardized Precipitation Index (SPI; McKee et al. 1993). Positive SPI values indicate greater than median precipitation and negative values indicate less than median precipitation (Bordi and Sutera 2002). The SPI is usually computed over multiple time scales ranging from 1 to 48 months, which reflects the impact of drought on the availability of different water resources. Among users, there is a general consensus about the fact that the SPI describes drought events affecting the agricultural practices during the shorter time scales (for example 3–6 months) While, on the longer ones (12–24 months), this procedure is more suitable for water resource management purposes (Raziei et al. 2009).

So, the present study describes the application of SPI for the determination of climatic drought at different time scales (3, 6, 9, 12, 18 and 24 months) in 42 synoptic stations of Iran within a 30-years period (1975–2005). Then, the SPI trend was determined at different time scales by Mann–Kendall non-parametric test. Our results can be applied, as a general perspective, to different aspects of natural resources management especially, water resource management.

2 Study area and data

Iran, with the area of 1648000 km², is located in the southwest of Middle East. In the most parts of country, four seasons are usually experienced although in general, a year can be divided into 2 seasons, summer and winter. Iran has various geographical, topographical and climatic conditions. Iran is surrounded by two mountain ranges namely Alborz to the north and Zagros to the west and the highest point of the country is located within the Alborz mountain range with an elevation of 5628 m above the mean sea level. These mountains avoid Mediterranean moisture-bearing systems from crossing through this region to the east. The Zagros mountain range is responsible for the major portion of rain-producing air masses that enter the region from the west and north-west, with relatively high amounts of rainfall (Sadeghi et al. 2002). The climate of this region is defined as sub-tropical with hot and dry weather in the summer season. The main cause of annual rainfall variability in Iran is the changing position of synoptic systems and year-to-year variation in the number of cyclones passing through the region (Modarres and Silva 2007).

The climate of a region is described by long-term averages, frequency and extremeness of several variables of weather, particularly the precipitation and temperature (Durdu 2010). The Iranian climate is arid and semiarid,

Table 1 Characteristics of surveyed stations

Station name	X coordinate	Y coordinate	Elevation (m)
Abadan	48.25	30.37	6.6
Abadeh	52.67	31.18	2030
Ahvaz	48.67	31.33	22.5
Arak	49.77	34.10	708
Ardebil	48.28	38.25	332
Babolsar	52.65	36.72	–21
Bam	58.35	29.10	66.9
Bandar abbas	56.37	27.22	9.8
Bandar anzali	49.47	37.47	–26.2
Bandar lenge	54.83	26.53	22.7
Birjand	59.20	32.87	1491
Bushehr	50.83	28.98	19.6
Chabahar	60.62	25.28	8
Esfahan	51.67	32.62	1550.4
Fasa	53.68	28.97	1288.3
Ghazvin	50.05	36.25	279.2
Gorgan	54.27	36.85	13.3
Hamedan	48.72	35.20	679.7
Iranshahr	60.70	27.20	591.1
Jask	57.77	25.63	5.2
Kashan	51.45	33.98	982.3
Kerman	56.97	30.25	1753
Kermanshah	47.15	34.35	318.6
Khoram abad	48.28	33.43	147.8
Khoy	44.97	38.55	103
Mashhad	59.63	36.27	999.2
Orumieh	45.08	37.53	1315.9
Rasht	49.60	37.25	–6.9
Sabzevar	57.72	36.20	977.6
Sanandaj	47.00	35.33	1373.4
Semnan	53.55	35.58	130.8
Shahrekord	50.85	32.28	48.9
Shahrud	54.95	36.42	345.3
Shiraz	52.60	29.53	484
Tabas	56.92	33.60	711
Tabriz	46.28	38.08	361
Tehran	51.32	35.68	190.8
Torbat heydarieh	59.22	35.27	1450.8
Yazd	54.28	31.90	1237.2
Zabol	61.48	31.03	489.2
Zahedan	60.88	29.47	1370
Zanjan	48.48	36.68	663

except the northern and western mountainous part of the country. In most of the regions of Iran, summer is warm-arid and winter is cold while the internal part bears continental climate. Temperature range (maximum and minimum), in most parts of the country, is about 22–26°C. The major part

Table 2 Different time series of SPI trends and M parameter of Mann–Kendall test in the mentioned synoptic stations

Station name	3 months	6 months	9 months	12 months	18 months	24 months
Abadan	-2.41 ^{-*}	-0.71	-0.72	-1.97 ^{-*}	-1.24	-2.73 ^{-***}
Abadeh	-1.76	-1.25	-1.06	-1.55	-1.19	-1.30
Ahvaz	-2.46 ^{-*}	-0.98	-1.29	-2.33 ^{-*}	-1.41	-2.05 ^{-*}
Arak	-1.37	-1.89	-2.88 ^{-***}	-4.63 ^{-***}	-4.32 ^{-***}	-5.83 ^{-***}
Ardebil	-1.84	-2.83 ^{-***}	-3.16 ^{-***}	-4.37 ^{-***}	-4.97 ^{-***}	-5.82 ^{-***}
Babolsar	0.28	0.39	0.73	1.40	1.11	0.87
Bam	-2.14 ^{-***}	-1.67	-2.78 ^{-**}	-3.64 ^{-***}	-4.13 ^{-**}	-4.86 ^{-***}
Bandar abbas	-3.55 ^{-***}	-3.26 ^{-***}	-4.35 ^{-***}	-5.84 ^{-***}	-6.37 ^{-***}	-7.16 ^{-***}
Bandar anzali	-0.67	-1.44	-3.01 ^{-***}	-4.97 ^{-***}	-3.89 ^{-**}	-6.66 ^{-***}
Bandar lenge	-5.79 ^{-***}	-4.03 ^{-***}	-5.07 ^{-***}	-5.79 ^{-***}	-5.61 ^{-**}	-6.17 ^{-***}
Birjand	-2.71 ^{-***}	-2.48 ^{-*}	-3.49 ^{-**}	-4.79 ^{-**}	-5.42 ^{-**}	-7.55 ^{-***}
Bushehr	-2.03 ^{-*}	0.86	2.21 ^{++*}	2.94 ^{+++*}	3.47 ^{+++*}	4.02 ^{+++*}
Chabahar	-6.84 ^{-***}	-4.77 ^{-***}	-5.27 ^{-**}	-6.64 ^{-***}	-7.15 ^{-**}	-7.64 ^{-***}
Esfahan	-1.01	-0.47	0.14	0.29	-0.02	1.64
Fasa	-2.35 ^{-*}	-0.97	-0.88	-1.62	-1.67	-2.19 ^{-*}
Ghazvin	-0.95	-1.19	-1.44	-0.98	-1.62	-1.97 ^{-*}
Gorgan	-1.77	-2.57 ^{-***}	-3.42 ^{-***}	-4.43 ^{-***}	-5.10 ^{-**}	-6.27 ^{-***}
Hamedan	-0.49	-0.51	-0.55	-0.04	0.21	1.19
Iranshahr	-4.31 ^{-***}	-4.61 ^{-***}	-4.84 ^{-**}	-5.12 ^{-**}	-5.21 ^{-**}	-4.80 ^{-***}
Jask	-7.37 ^{-***}	-5.83 ^{-***}	-7.39 ^{-**}	-9.76 ^{-***}	-8.14 ^{-**}	-8.59 ^{-***}
Kashan	-0.78	-0.22	0.13	0.14	0.44	0.25
Kerman	-1.54	-1.40	-1.78	-3.10 ^{-***}	-2.99 ^{-**}	-4.32 ^{-***}
Kermanshah	-1.28	-1.15	-1.56	-2.77 ^{-**}	-1.92	-2.25 ^{-*}
Khoram abad	-1.30	-1.50	-2.39 ^{-***}	-4.27 ^{-***}	-3.38 ^{-**}	-5.59 ^{-***}
Khoy	-3.71 ^{-***}	-5.63 ^{-***}	-7.04 ^{-**}	-9.19 ^{-**}	-9.94 ^{-**}	-12.05 ^{-***}
Mashhad	-1.10	-2.07 ^{-*}	-3.47 ^{-**}	-4.84 ^{-**}	-5.88 ^{-**}	-7.86 ^{-***}
Orumieh	-2.87 ^{-***}	-4.19 ^{-***}	-5.87 ^{-**}	-7.52 ^{-**}	-7.62 ^{-**}	-9.39 ^{-***}
Rasht	0.44	-0.28	-1.00	-1.35	-0.83	-1.36
Sabzevar	-1.77	-2.16 ^{-*}	-3.45 ^{-**}	-4.79 ^{-**}	-4.86 ^{-**}	-7.12 ^{-***}
Sanandaj	-3.52 ^{-***}	-4.75 ^{-***}	-7.74 ^{-**}	-10.61 ^{-***}	-10.14 ^{-**}	-13.02 ^{-***}
Semnan	-0.55	-0.70	-0.84	-0.94	-1.32	-2.17 ^{-*}
Shahrekord	-1.14	-1.22	-1.75	-2.43 ^{-*}	-2.63 ^{-**}	-3.17 ^{-***}
Shahrud	-2.06 ^{-*}	-2.74 ^{-***}	-3.79 ^{-**}	-4.98 ^{-**}	-5.13 ^{-**}	-6.88 ^{-***}
Shiraz	-1.60	-0.11	0.86	1.21	1.37	1.79
Tabas	-2.57 ^{-***}	-0.90	-0.65	-0.88	-0.89	-0.92
Tabriz	-2.23 ^{-*}	-3.20 ^{-***}	-4.42 ^{-**}	-6.31 ^{-***}	-7.03 ^{-**}	-8.58 ^{-***}
Tehran	-0.25	-0.41	-0.18	0.58	-0.75	-1.29
Torbat heydarieh	-0.73	-1.17	-1.92	-3.22 ^{-***}	-2.87 ^{-**}	-3.39 ^{-***}
Yazd	-3.09 ^{-***}	-3.12 ^{-***}	-4.46 ^{-**}	-6.26 ^{-***}	-7.31 ^{-**}	-11.07 ^{-***}
Zabol	-4.88 ^{-***}	-1.51	-0.85	-0.35	-0.56	-1.44
Zahedan	-3.18 ^{-***}	-2.18 ^{-*}	-2.49 ^{-*}	-2.93 ^{-***}	-2.78 ^{-**}	-2.61 ^{-***}
Zanjan	-1.43	-2.16 ^{-*}	-3.22 ^{-***}	-4.19 ^{-**}	-4.60 ^{-**}	-5.75 ^{-***}

In this table ⁺** and ⁺*** indicate the significant upward trend at $\alpha = 0.05$ and 0.01 , respectively and ⁻* and ⁻** indicate the significant negative trends at $\alpha = 0.05$ and 0.01 , respectively

of precipitation occurs between the months of November to May and then the warm-dry season prevails. The mean annual precipitation is about 240 mm in Iran and most of which occurs in the plains of northern Alborz mountain

range. While, Caspian Seaside and Zagros Mountain range receive the precipitation of about 1800 and 480 mm, respectively. Toward the central part and east of Iran, the precipitation decreases up to 100 mm or less.

Table 3 The b coefficients for linear trend of different monthly-time scales

Station name	3 months	6 months	9 months	12 months	18 months	24 months
Abadan	0.00	-0.01	-0.01	-0.01	-0.01	-0.01
Abadeh	-0.01	-0.01	-0.01	-0.01	-0.01	-0.01
Ahvaz	0.00	-0.01	-0.01	-0.01	-0.01	-0.01
Arak	-0.01	-0.01	-0.02	-0.03	-0.03	-0.03
Ardebil	-0.01	-0.02	-0.02	-0.03	-0.03	-0.04
Babolsar	0.00	0.00	0.00	0.01	0.01	0.01
Bam	-0.01	-0.01	-0.02	-0.02	-0.03	-0.03
Bandar abbas	-0.01	-0.02	-0.03	-0.03	-0.04	-0.05
Bandar anzali	-0.01	-0.01	-0.02	-0.03	-0.03	-0.05
Bandar lenge	-0.01	-0.02	-0.03	-0.04	-0.04	-0.04
Birjand	-0.01	-0.01	-0.02	-0.04	-0.04	-0.05
Bushehr	0.00	0.00	0.01	0.02	0.03	0.04
Chabahar	-0.02	-0.02	-0.03	-0.04	-0.04	-0.04
Esfahan	0.00	0.00	0.00	0.00	0.00	0.00
Fasa	-0.01	-0.01	-0.01	-0.01	-0.01	-0.01
Ghazvin	-0.01	-0.01	-0.01	-0.01	-0.01	-0.02
Gorgan	-0.01	-0.01	-0.02	-0.03	-0.03	-0.04
Hamedan	0.00	0.00	0.00	0.00	0.00	0.00
Iranshahr	-0.02	-0.03	-0.03	-0.04	-0.04	-0.05
Jask	-0.02	-0.03	-0.04	-0.05	-0.05	-0.06
Kashan	0.00	0.00	0.00	0.00	0.00	0.01
Kerman	-0.01	-0.01	-0.01	-0.02	-0.02	-0.03
Kermanshah	-0.01	-0.01	-0.01	-0.02	-0.01	-0.02
Khoram abad	-0.01	-0.01	-0.01	-0.03	-0.02	-0.03
Khoy	-0.02	-0.03	-0.04	-0.06	-0.06	-0.07
Mashhad	-0.01	-0.01	-0.02	-0.04	-0.04	-0.05
Orumieh	-0.02	-0.03	-0.03	-0.04	-0.04	-0.05
Rasht	0.00	0.00	-0.01	-0.01	-0.01	-0.01
Sabzevar	-0.01	-0.01	-0.02	-0.03	-0.03	-0.04
Sanandaj	-0.01	-0.03	-0.05	-0.06	-0.06	-0.08
Semnan	0.00	0.00	-0.01	-0.01	-0.01	-0.02
Shahrekord	-0.01	-0.01	-0.01	-0.02	-0.02	-0.02
Shahrud	-0.01	-0.02	-0.02	-0.03	-0.03	-0.03
Shiraz	0.00	0.00	0.00	0.01	0.01	0.02
Tabas	-0.01	-0.01	-0.01	-0.01	-0.01	-0.01
Tabriz	-0.01	-0.02	-0.03	-0.04	-0.04	-0.05
Tehran	0.00	0.00	0.00	0.00	-0.01	-0.01
Torbat heydarieh	0.00	-0.01	-0.01	-0.02	-0.02	-0.03
Yazd	-0.01	-0.02	-0.03	-0.04	-0.04	-0.06
Zabol	0.00	0.00	-0.01	-0.01	-0.01	-0.01
Zahedan	-0.01	-0.01	-0.01	-0.02	-0.02	-0.02
Zanjan	0.00	-0.01	-0.02	-0.03	-0.03	-0.04
Mean of b coefficients	-0.01	-0.01	-0.02	-0.02	-0.02	-0.03

Most parts of Iran are affected by subtropical high air masses in the summer season. It causes the existence of hot summers in the country. The major amount of precipitation is produced by Mediterranean air masses, brought in with

the western winds in the winters. The location of 42 synoptic meteorological stations is displayed in the map of Iran (Fig. 1). These meteorological stations have a reasonable distribution with acceptable period of meteorological data

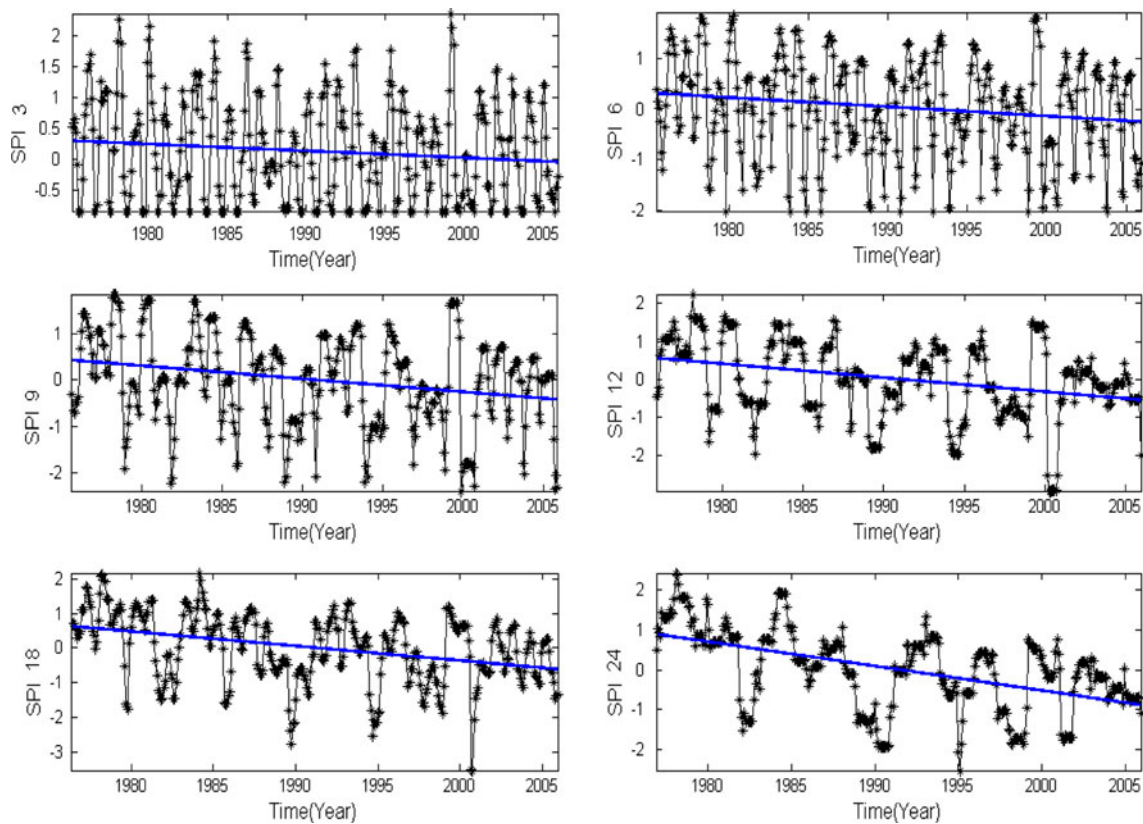


Fig. 2 Different time series (3, 6, 9, 12, 18 and 24 monthly SPI) for the synoptic meteorological station of Yazd

(31 years), which can support the studies of climatic variations from two aspects; spatial and temporal, within recent decades. Table 1 indicates general characteristics of elevation, latitude and longitude of the 42 surveyed stations.

The precipitation data, analyzed during the present study, were collected from the Iran Meteorological Data site (<http://www.weather.ir>). Data were downloaded at a monthly time scale and then different time series of precipitation were derived from this information.

3 Methods

3.1 Mann–Kendall non-parametric test

The popular non-parametric rank-based Mann–Kendall test (Sneyers 1990) is particularly useful for detecting trends in the paired data, as: (i) the data that do not need to be conformed to particular distribution, thus extreme values are acceptable (Hirsch et al. 1993), (ii) when missing values are allowed (Yu et al. 1993), or (iii) when the use of relative magnitudes (ranking), rather than the numerical values, allows ‘trace’ or ‘below detection limit’ data to be used—they are assigned a value lesser than that of the smallest measured one, and (iv) in time series analysis, it is unnecessary to specify whether the trend is linear or not

(Sneyers 1990; Yu et al. 1993; Silva 2005). The correlation between two variables is termed as the Kendall’s correlation coefficient or Kendall statistics.

Consider a time series $\{X_i | i = 1, 2, \dots, N\}$ with the record length of N . According to Salas (1993) and Yu et al., (1993), the null hypothesis H_0 states that the deseasonalized data $\{X_i\}$ are a sample of “ n ” independent and identically distributed random variables. The alternative hypothesis (H_1) of a two-sided test is that the distributions of X_i and X_j are not identical for $i, j \leq N$ with $i \neq j$. Each value of $X_i, i = 1, \dots, N - 1$ is compared with subsequent values of $\{X_j | j = i + 1, i + 2, \dots, N\}$ and the sum of times of $X_i > X_j$. The number of positive differences for all the considered differences (p) is given by:

$$p = \sum_i n_i,$$

The Mann–Kendall statistics (S) is calculated as:

$$S = \left(\frac{4p}{N(N-1)} \right) - 1,$$

where p is the number of positive differences for all the differences considered. Under the H_0 hypothesis, the distribution of S is normal within the limit of $N \rightarrow \infty$ (Yu et al. 1993). The mean and variance of S are calculated as:

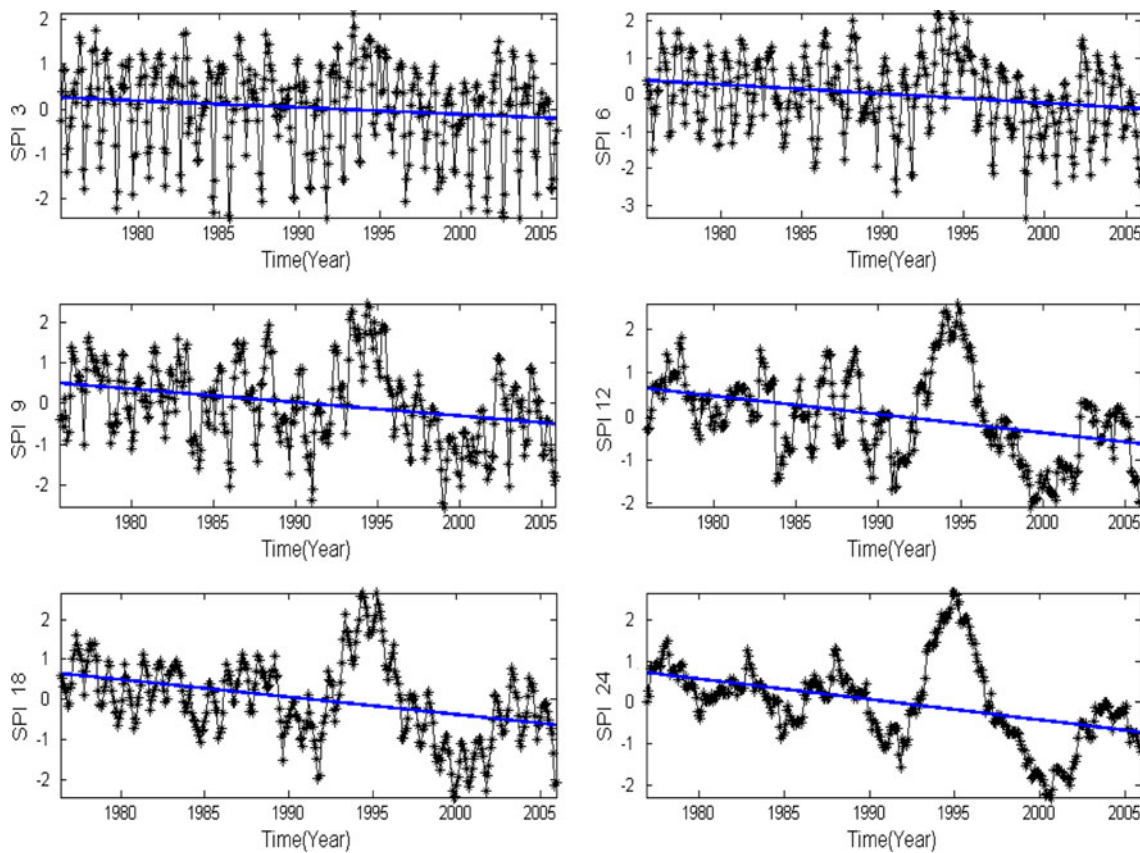


Fig. 3 Different time series (3, 6, 9, 12, 18 and 24 monthly SPI) for the synoptic meteorological station of Orumieh

$$E(S) = 0,$$

$$Var(S) = 2(2N + 5)/(9N(N - 1)),$$

For $N > 10$, the test is conducted using a normal approximation (Hirsch et al. 1993). The standardized test statistics (M) is calculated as:

$$M = S/(Var(s))^{1/2}$$

Hisdal et al. (2001) accentuated that the hypothesis (H_1) of an upward or downward trend cannot be rejected at the significance level of α if $|M| > M_{(1-\alpha/2)}$, where $M_{(1-\alpha/2)}$ is $1 - \alpha/2$ quintile of the standard normal distribution. When a positive value of M indicates an upward trend, its negative value shows a downward trend. $|M| > 1.96$ indicates a significant upward/downward trend (at a significance level of $\alpha = 0.05$) and $|M| > 2.576$ indicates an extremely significant trend (at a significance level of $\alpha = 0.01$) (Zhai and Feng 2008). In this paper, after deriving the Mann–Kendall statistical test, M of all the mentioned time-scale data series was calculated at a significance level of $\alpha = 0.05$.

3.2 Standardized Precipitation Index (SPI)

The SPI is widely accepted and used throughout the world in both research and operational management since it is

normalized to a location and time (Wu et al. 2007). The SPI is computed by fitting a probability density function to the frequency distribution of precipitation summed over the time scale of interest. This is performed separately for each month (or any other temporal basis of the raw precipitation time series) and for each location in space. Each probability density function is then transformed into a standardized normal distribution (Mishra and Desai 2005). The gamma distribution is defined by its probability density function as:

$$g(x) = \frac{1}{\beta^\alpha \Gamma(\alpha)} x^{\alpha-1} e^{-x/\beta} \quad \text{for } x > 0$$

where $\alpha > 0$ is a shape factor, $\beta > 0$ is a scale factor, and $x > 0$ is the amount of precipitation. $\Gamma(\alpha)$ is the gamma function, which is defined as:

$$\Gamma(\alpha) = \int_0^\infty y^{\alpha-1} e^{-y} dy$$

Fitting the distribution to the data requires that α and β be estimated. For this, Edwards and McKee (1997) have suggested a method using the approximation of Thom (1958) for maximum likelihood as follows (for n observations):

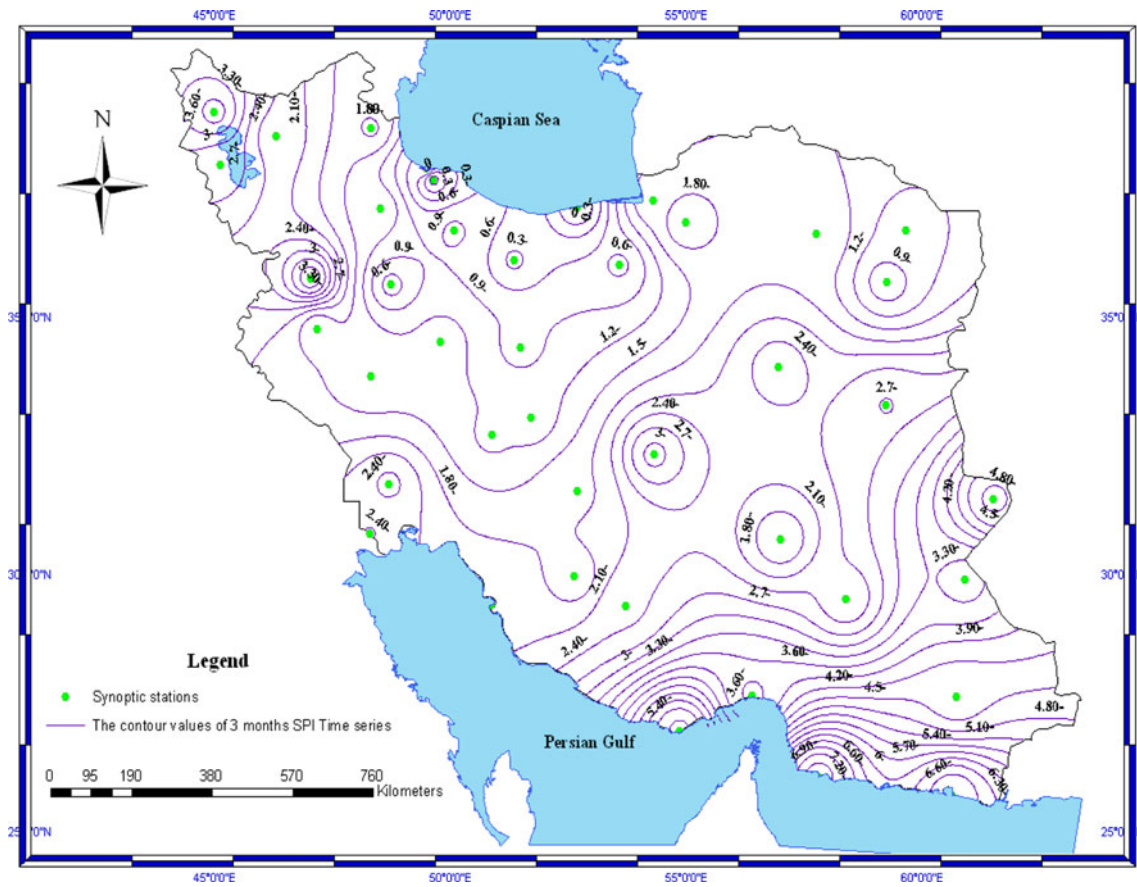


Fig. 4 Spatial distribution of M parameter of Mann–Kendall test at different places of Iran during 3 months SPI time series

$$\alpha = \frac{1}{4A} \left(1 + \sqrt{1 + \frac{4A}{3}} \right)$$

$$\beta = \frac{\bar{x}}{\alpha}$$

where

$$A = \ln(\bar{x}) - \frac{1}{n} \sum_{i=1}^n \ln(x_i)$$

The resulting parameters are then used to find the cumulative probability of an observed precipitation event for the given month or any other time scale:

$$G(x) = \int_0^x g(x)dx = \frac{1}{\beta^\alpha \Gamma(\alpha)} \int_0^x x^{\alpha-1} e^{-x/\beta} dx$$

Letting $t = x/\beta$; this equation becomes the incomplete gamma function

$$G(x) = \frac{1}{\Gamma(\alpha)} \int_0^x t^{\alpha-1} e^{-t} dt$$

Since, the gamma function is undefined for $x = 0$ and a precipitation distribution may contain zeros, the cumulative probability becomes:

$$H(x) = q + (1 - q)G(X)$$

where q is the probability of zero precipitation. The cumulative probability, $H(x)$ is then transformed to the standard normal random variable Z with the mean equal to zero and the variance of one, which is the value of SPI. Following Edwards and McKee (1997) and Hughes and Saunders (2002), an approximate conversion is used in this study, as provided by Abramowitz and Stegun (1965) in the form of an alternative:

$$Z = \text{SPI} = - \left(t - \frac{c_0 + c_1 t + c_2 t^2}{1 + d_1 t + d_2 t^2 + d_3 t^3} \right)$$

for $0 < H(X) < 0.5$

and

$$Z = \text{SPI} = t - \frac{c_0 + c_1 t + c_2 t^2}{1 + d_1 t + d_2 t^2 + d_3 t^3}$$

for $0.5 < H(X) < 1.0$

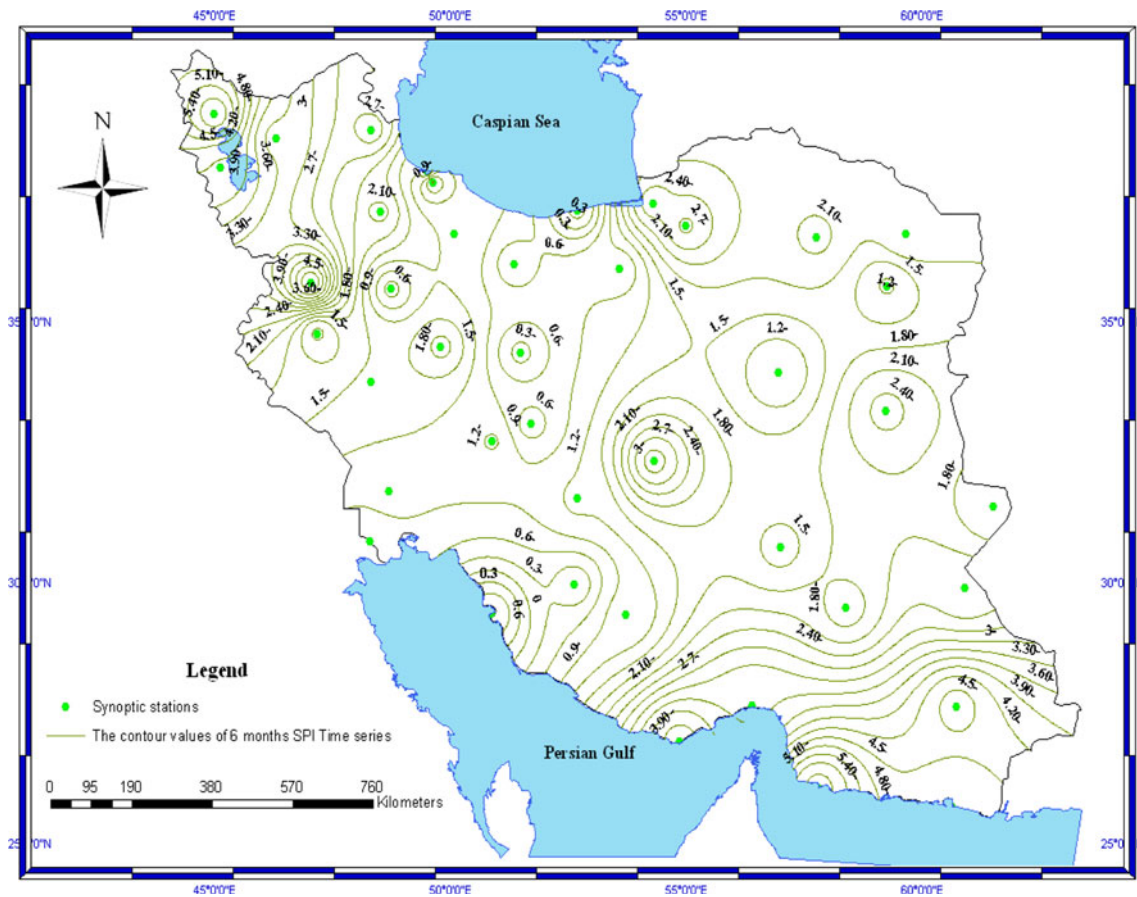


Fig. 5 Spatial distribution of M parameter of Mann–Kendall test at different places of Iran during 6 months SPI time series

where

$$t = \sqrt{\ln\left(\frac{1}{H(X)^2}\right)} \quad \text{for } 0 < H(X) < 0.5$$

and

$$t = \sqrt{\ln\left(\frac{1}{(1-H(X))^2}\right)} \quad \text{for } 0.5 < H(X) < 1.0$$

and $c_0 = 2.515517$, $c_1 = 0.802853$, $c_2 = 0.010328$, $d_1 = 1.432788$, $d_2 = 0.189269$ and $d_3 = 0.001308$ (Mishra and Desai 2005).

During the present study, the calculations of SPI and the Mann–Kendall test (M) were performed by MATLAB software.

The first order equation, $Y = bx + a$, is used in different time series. The negative sign of b coefficient clearly shows the negative trend. While, the positive sign indicates a positive trend of sequences. On the other hand, the amount of b coefficient shows the intensity of changes. Table 3 represents the b coefficients of different time series in SPI analysis. The results of ‘M’ parameter in Mann–Kendall

test, demonstrated in Table 2, are used for the spatial analysis of SPI trend at different time scales in the map of Iran.

4 Results

Table 2 indicates the monthly survey of SPI trends within the mentioned synoptic stations. As shown in the table, many stations have faced significant negative trends. While, the positive-significant trends are rare in some stations such as; Bushehr. On the other hand, it is considerable that for many stations, absolute value of M shows an increase with the increase in time scale. For making the results brief, the details of significance of each station and the time series are avoided during the present study. Therefore, the results are mostly explained in the form of presented maps of the trends for different SPI time series in Iran.

Table 3 indicates the b coefficient of trend of each station and each surveyed time series. The recent results are similar to those of M parameter in Mann–Kendall test, as presented in Table 2, which shows that the negative signs

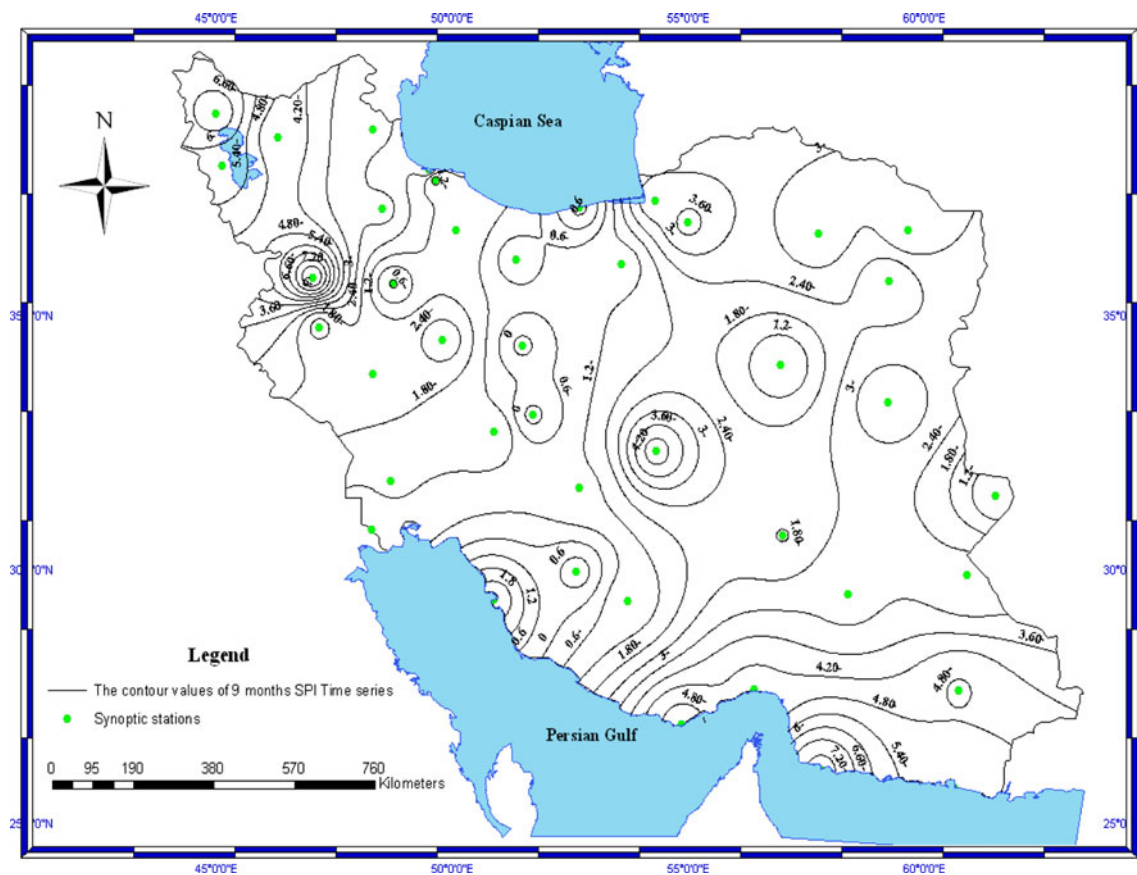


Fig. 6 Spatial distribution of M parameter of Mann–Kendall test at different places of Iran during 9 months SPI time series

of SPI trend at different time series are considerable. Negative sign indicates the negative trend of SPI series. On the other hand, common to the results of M parameter in Mann–Kendall test, it is considerable that when the time scale of a station is increased, the absolute value of b coefficient increases too. In the final row of Table 2, the mean of b coefficients is presented at different time series. As mentioned above, for the 24-months SPI time series, the absolute value of b coefficient increased. According to these averages, the average slopes 3 and 6 months time series are recorded to be -0.01 and 9 , respectively. While, those of 12 and 18 months were -0.02 and, of 24 months were observed to be -0.03 , respectively, in Iran.

Figures 2 and 3 indicate different time series (3, 6, 9, 12, 18 and 24 months' SPI) for 2 selected meteorological stations of Yazd and Orumieh. According to these figures, the first order fitted line shows each time series. The Figs. 2 and 3 also show the negative trend of each time series and the increasing steepness of the fitted curves (or the b coefficient amounts) when time series is increased.

Figures 4, 5, 6, 7, and 8 indicate the spatial distribution of M parameter in Mann–Kendall test at different places of Iran in different time series. Figure 4 shows SPI trend

values for 3 months time series. As shown in Fig. 4, there is no considerably significant trend around of Caspian Sea and north east of the country while other boundary areas, especially south east parts, show a considerably negative 3-months SPI time series. It can be determined by the Fig. 4 that more than half of the country has faced a negative trend of 3 months SPI time series.

Figure 5 shows a 6 months SPI time series. Similar to the 3 months SPI map (Fig. 4), the north of Iran around the Caspian Sea shows no significant trend like some of the north-eastern regions and south-western regions in the north of Persian gulf. While, significant trend were recorded in the southeast, south and north-western regions. Similar results can be seen for 9 months SPI time series map of Fig. 6. As shown in the figure, the north-eastern parts have a significant downward trend.

Figure 7 shows the distribution of M parameter of Mann–Kendall test for the 18 months time series. In this figure, it can be seen that the absolute values of M parameter are more considerable as compared to those of the previously mentioned ones. The regions around the Caspian Sea and the southwestern part had non-significant trend. These results are presented in the Figs. 7 and 8 for

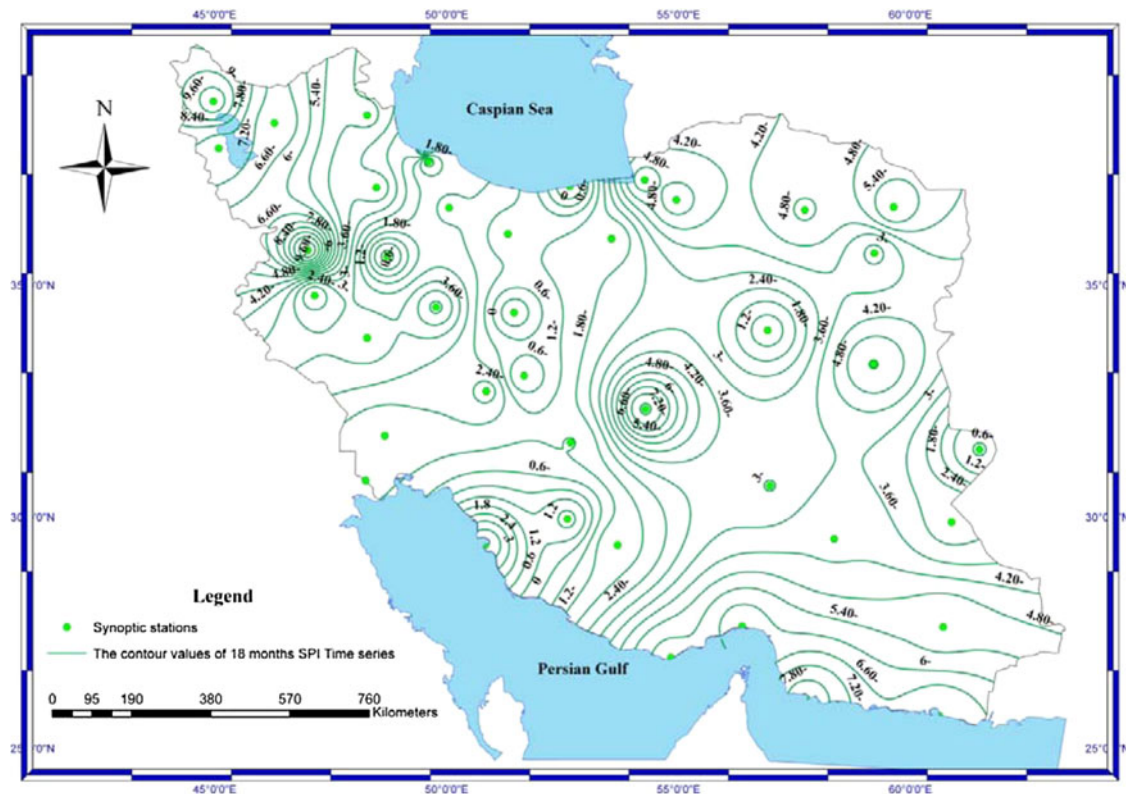


Fig. 7 Spatial distribution of M parameter of Mann–Kendall test at different places of Iran during 18 months SPI time series

monthly SPI time series of 18 and 24 months, respectively. Therefore, for these time series, it can be found that significantly negative trends can be experienced in whole country except the south-western part in the north of Persian Gulf.

5 Discussion and conclusion

This study describes the climatic drought trend in Iran between 1975 and 2005. Drought has been a recurrent phenomenon in Iran for the last several decades. SPI was used for this study which is based on the consideration that each component of a water resources system reacts to a deficit in precipitation over different time scales (Tsakiris et al. 2007). This study has focused on different and important time scales of 3, 6, 9, 12, 18 and 24 months. In general, the significantly negative SPI trend means the increase of number and the intensification of climatic drought condition as well. It is clear that positive trend of SPI amounts means the better condition related to drought. In fact, positive amounts mean that the numbers of positive SPI with more amounts are considerable in the sequence of SPI values. While the negative trend means that there are more numbers of negative SPI with lesser amounts are

considerable. Results indicate that the southeast, west, and northwest parts of Iran have faced a negative trend of SPI i.e., more frequent and intense drought. This situation can strongly affect the water resources and their management in these regions.

In condition of increasing of the drought, water resource management strategies must be adjusted according to the changing trends in rainfall and the spatial patterns of drought frequency. With attention to agricultural activities that performed in the warm seasons (spring and summer) and the lack of water resources in this period as well as the downward trend in the SPI values, more attention should be paid to drought trends during the agricultural development decision-making process in Iran.

On the other hand, the present results show that the absolute values of M and coefficient ‘b’ increased during the 24-months SPI series. The SPI analysis has some limitations, which include its inability to define drought in the extremely low precipitation areas at shorter time scales, where a zero or a small amount of droughts occurred for the entire time period using the 1-month and occasionally 3-months SPI test. This was the result of precipitation median for these areas, for the periods on record, being zero. When the time scales increased and more months considered, this problem was solved (Kangas and Brown

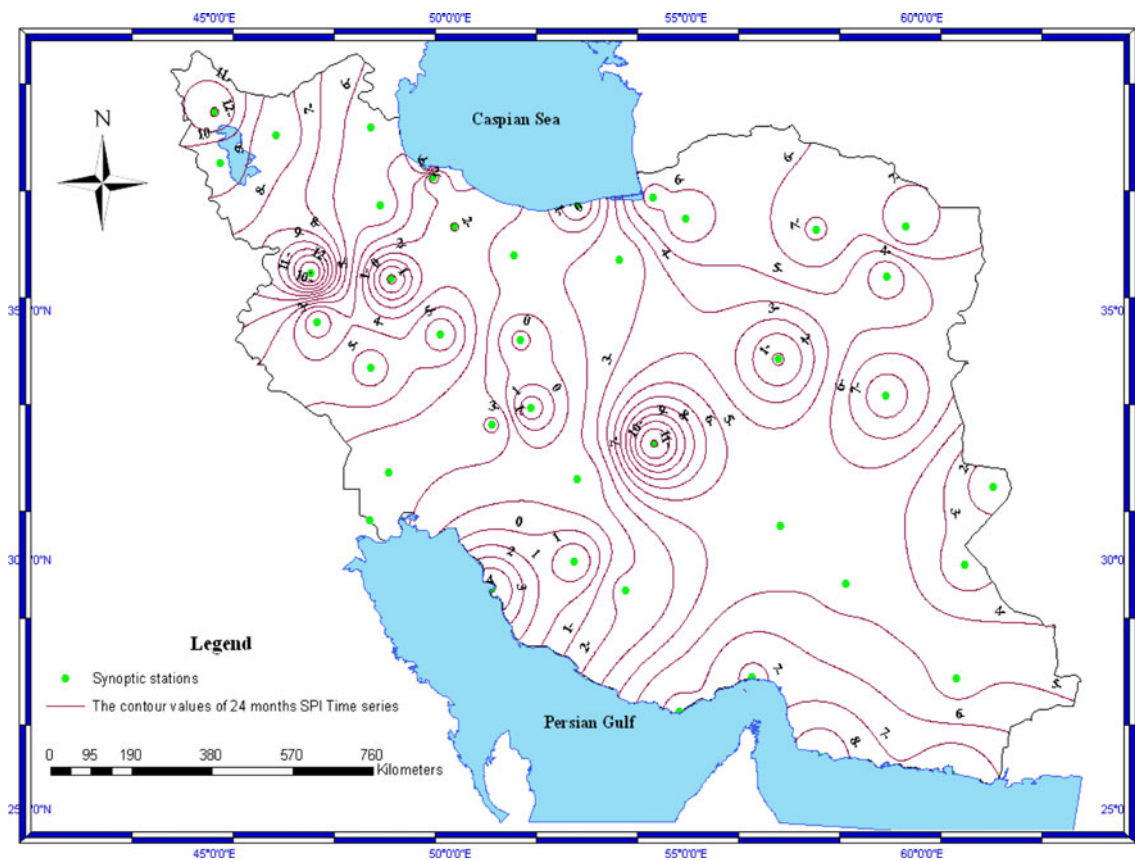


Fig. 8 Spatial distribution of M parameter of Mann–Kendall test at different places of Iran during 24 months SPI time series

2007). On the other hand, because of data limitations, time scales more than 24 months may be unreliable (Guttman 1999). It can be said that lesser M parameter or b coefficient at lower time series are related to the limitation of application of 3 months SPI series for arid and semiarid regions. On the other hand, with the increase in the months of SPI time series, the curves become smoother and the crenulations can be decreased. So, in this condition, the general trend of sequence or time series is more obvious and detectable by some functions such as Mann–Kendall test or first order fitting.

After the survey of different climatic stations, it can be said that the number and intensification of climatic drought events is considerable in Iran and needs the detection and analysis of future SPI trend at different stations of Iran. Perhaps, the non-significantly negative SPI trends could be a warning of significantly negative ones in the future. However, more research is needed to forecast the SPI trend at different time scales and in different regions of Iran.

Indeed According to results it is very hard to say that the climate change has affected increasing of the drought in Iran except that the significant relation between temperature increasing and increasing of drought is found. Further studies can be dedicated to the relationship between SPI

trend and other climatic parameters such as temperature, relative humidity and precipitation trend during the last decades. Also it may be useful to analyze the relationship between drought trends and other climatic parameters under global warming conditions and this is our aim for future studies. This is because the study of drought and drought trend under the conditions of global warming and climate change is very important and considerable in Iran, as the country is faced with water shortage in most regions, and global warming may intensify the problem.

Anyway increasing of the drought certainly affects the agricultural production in arid and semiarid regions such as Iran. Water resources limitation is one of the most important restrictions in agricultural productions improvement in arid and semiarid regions of Iran. So, more drought means more limitation and shortage related to water resources and therefore, this affects agricultural yields.

In addition, Water resources management strategies must be adjusted according to changing trends in rainfall and the spatial patterns of drought frequency. For the most part of Iran, such changes in precipitation are detrimental to agricultural production and ecosystem rehabilitation in arid and semiarid regions. In particular, the southeast regions of the Iran require a more efficient measurement of

regulation to manage water resources and meet the requirements of agricultural and drinking water supply.

The trend of precipitation in the arid regions especially in the southeast part of Iran, may tend to accelerate desertification and increase the frequency of sandstorms in the future.

In condition of increasing of the drought, more attention should be focused on precipitation trends and drought distribution during the agricultural development decision-making process and drought hazards mitigation.

Acknowledgment The authors greatly acknowledge the financial support of Payame Noor University, Yazd, Iran for running the present project.

References

- Abramowitz M, Stegun A (1965) Handbook of mathematical formulas graphs and mathematical tables. Dover Publications Inc, New York
- Akhtari R, Morid S, Mahdian MH, Smakhtin V (2009) Assessment of areal interpolation methods for spatial analysis of SPI and EDI drought indices. *Int J Climatol* 29:135–145
- Bonaccorso B, Cancelliere A, Rossi G (2003) An analytical formulation of return period of drought severity. *Stochast Environ Res Risk Assess* 17:157–174
- Bordi I, Sutera A (2002) An analysis of drought in Italy in the last fifty years. *Nuovo Cimento* 25C:185–206
- Durdu ÖF (2010) Application of linear stochastic models for drought forecasting in the Büyük Menderes river basin, western Turkey. *Stochast Environ Res Risk Assess* 24:1145–1162
- Edwards DC, McKee TB (1997) Characteristics of 20th century drought in the United States at multiple timescales. *Climatology Report No. 97-2*. Colorado State University, Fort Collins
- Guttman NB (1999) Accepting the Standardized Precipitation Index: a calculation algorithm. *J Am Water Resour Assoc* 35(2):311–322
- Hirsch R, Helsel D, Cohn T, Gilroy E (1993) Statistical analysis of hydrologic data. In: Maidment D (ed) *Handbook of hydrology*. McGraw-Hill, New York
- Hisdal H, Stahl K, Tallaksen LM, Demuth S (2001) Have streamflow droughts in Europe become more severe or frequent? *Int J Climatol* 21:317–333
- Hughes BL, Saunders MA (2002) A drought climatology for Europe. *Int J Climatol* 22:1571–1592
- Kangas R, Brown T (2007) Characteristics of US drought and pluvials from a high-resolution spatial dataset. *Int J Climatol* 27:1303–1325
- Łabędzki L (2007) Estimation of local drought frequency in central Poland using the Standardized Precipitation Index SPI. *Irrig Drain* 56:67–77
- McKee TB, Doesken NJ, Kleist J (1993) The relationship of drought frequency and duration to time scales. In: Preprints, 8th conference on applied climatology, Anaheim, CA, 17–22 January 1993, pp 179–184
- Mishra AK, Desai VR (2005) Drought forecasting using stochastic models. *Stochast Environ Res Risk Assess* 19:326–339
- Mishra AK, Singh VP, Desai VR (2009) Drought characterization: a probabilistic approach. *Stochast Environ Res Risk Assess* 23:41–55
- Modarres R (2007) Streamflow drought time series forecasting. *Stochast Environ Res Risk Assess* 21:223–233
- Modarres R, VPR Silva (2007) Rainfall trends in arid and semi-arid regions of Iran. *J Arid Environ* 70:344–355
- Morid S, Smakhtin S, Moghaddasi M (2006) Comparison of seven meteorological indices for drought monitoring in Iran. *Int J Climatol* 26:971–985
- Nadarajah S (2009) A bivariate pareto model for drought. *Stochast Environ Res Risk Assess* 23:811–822
- Palmer WC (1965) Meteorological drought. Research Paper No. 45. US Department of Commerce, Weather Bureau, Washington
- Paulo A, Pereira L (2006) Drought concepts and characterization: comparing drought indices applied at local and regional scales. *Water Int* 31(1):37–49
- Rahimzadeh Bajgiran P, Darvishsefat AA, Khalili A, Makhdoum MF (2008) Using AVHRR-based vegetation indices for drought monitoring in the Northwest of Iran. *J Arid Environ* 72:1086–1096
- Raziei T, Bordi I, Pereira LS (2008) A precipitation-based regionalization for Western Iran and regional drought variability. *Hydrol Earth Syst Sci* 12:1309–1321
- Raziei T, Saghafian B, Paulo AA, Pereira LS, Bordi I (2009) Spatial and temporal variability of drought in western Iran. *Water Resour Manag* 23:439–455
- Raziei T, Bordi I, Pereira LS (2010) An application of GPCC and NCEP/NCAR datasets for drought variability analysis in Iran. *Water Resour Manage*. doi:10.1007/s11269-010-9657-1
- Sadeghi AR, Kamgar-Haghighi AA, Sepaskahah AR, Khalili D, Zand-Parsa S (2002) Regional classification for dryland agriculture in southern Iran. *J Arid Environ* 50:333–341
- Salas JD (1993) Analysis and modeling of hydrologic time series. In: Maidment DR (ed) *Handbook of hydrology*. McGraw Hill, New York, pp 19.1–19.72
- Silva V (2005) On climate variability in Northeast of Brazil. *J Arid Environ* 58(4):575–596
- Sneyers R (1990) On the statistical analysis of series of observations. WMO Technical Note 43. World Meteorological Organization, Geneva
- Soleimmi K, Ramezani N, Ahmadi MZ, Bayat F (2005) Drought and rainfall trend analysis in Mazandaran watershed. *Khazar Agric Nat Resour* 1(3):1–28
- Tate E, Gustard A (2000) Drought definition: a hydrological perspective. In: Vogt J, Somma F (eds) *Drought and drought mitigation in Europe*. Kluwer, Dordrecht, pp 23–48
- Thom HCS (1958) A note on gamma distribution. *Monthly Weather Rev* 86:117–122
- Tsakiris G, Pangalou D, Vangelis H (2007) Regional drought assessment based on the Reconnaissance Drought Index (RDI). *Water Resour Manag* 21(5):821–833
- Wilhite DA (2000) Droughts as a natural hazard: concepts and definitions. In: *Drought: a global assessment*. Routledge, London, pp 3–18
- Wilhite DA, Glantz MH (1985) Understanding the drought phenomenon: the role of definitions. *Water Int* 10:111–120
- Wu H, Svoboda M, Hayes M, Wilhite D, Wen F (2007) Appropriate application of the Standardized Precipitation Index in arid locations and dry seasons. *Int J Climatol* 27:65–79
- Yazdani S, Kianirad A (2004) Revenue insurance: a new program for agricultural risk management agricultural economics and development. *Sci Res Q J* 12(3):47–68
- Yu Y, Zou S, Whittemore D (1993) Non-parametric trend analysis of water quality data of rivers in Kansas. *J Hydrol (Amst)* 150:61–80
- Zhai L, Feng Q (2008) Spatial and temporal pattern of precipitation and drought in Gansu Province, Northwest China. *Nat Hazards* 49(1):1–24